Biochemistry

 Volume 34, Number 9 March 7, 1995

Accelerated Publications

The Energetics and Dynamics of Molecular Recognition by Calmodulin†

Mark R. Ehrhardt, Jeffrey L. Urbauer, and A. Joshua Wand*

Department of Biochemistry, University of Illinois at Urbana−Champaign, 600 South Mathews Avenue, Urbana, Illinois 61801

Received November 30, 1994; Revised Manuscript Received January 18, 1995®

ABSTRACT: Amide hydrogen exchange has been used to examine the structural dynamics and energetics of the interaction of a peptide corresponding to the calmodulin binding domain of smooth muscle myosin light chain kinase with calcium-saturated calmodulin. Heteronuclear NMR $^{15}N-^{1}H$ correlation techniques were used to quantitate amide proton exchange rates of both ^{15}N-labeled and unlabeled amide protons of the smMLCK peptide complexed to calmodulin. Hydrogen exchange slowing factors were determined for 18 of the 19 amide hydrogens and found to span 6 orders of magnitude. The first six residues of the bound peptide were found to have slowing factors near 1 and are considered not to be hydrogen bonded, consistent with the previously reported model for the structure of the peptide. The pattern of hydrogen exchange of hydrogen-bonded amide hydrogens is indicative of end-fraying behavior characteristic of helix−coil transitions. The effective statistical mechanical parameters revealed by the end fraying are consistent with exchange from a highly solvated state. However, the slowing factors of the first hydrogen-bonded amide hydrogens are large, indicating the requirement for a reorganization of the calmodulin−peptide complex before the helix−coil transitions leading to exchange can occur. Taken together, these observations suggest that the collapsed complex reorganizes with an associated free energy change of 5.5 kcal/mol to a more open state where the helical peptide is highly solvated and undergoes helix−coil transitions leading to exchange. The free energy difference between the most and least stable intrahelical amide hydrogen bonds of the bound peptide is estimated to be approximately 2.5 kcal/mol. In reverse, these events are effectively those of the collapse of the initial encounter complex to the final stable complex structure. The results presented demonstrate the potential of hydrogen exchange for studying the dynamics and energetics of interprotein interactions along the free energy path from the initial encounter complex to the final equilibrium structure.

While high-resolution X-ray crystallographic and NMR techniques can provide precise details of equilibrium structures of proteins, the dynamics of the transitions between the potentially numerous transient conformational states remain in most cases unclear. This sentiment has recently been reiterated with respect to calmodulin and especially the complexes formed between calmodulin and its protein and peptide targets (Török & Whitaker, 1994). Calmodulin has been found to regulate a wide range of cellular targets and is consequently central to control of a number of critical cellular events (O'Neil & DeGrado, 1990). In the crystal, calcium-saturated calmodulin (CaM)[1] has two globular

† Supported by Research Grant DK-39806 from the National Institutes of Health.

* To whom correspondence should be addressed.

® Abstract published in *Advance ACS Abstracts*, February 15, 1995.

[1] Abbreviations: CaM, calcium-saturated calmodulin; HSQC, heteronuclear single-quantum coherence; NMR, nuclear magnetic resonance; NOE, nuclear Overhauser effect; NOESY, NOE-correlated spectroscopy, pH*, pH uncorrected for the isotope effect; smMLCKp, N-terminal acetylated and C-terminal amidated peptide with sequence corresponding to the calmodulin binding domain of the smooth muscle myosin light chain kinase.

0006-2960/95/0434-2731$09.00/0

domains separated by a long α helix (Babu et al., 1988). Chemical cross-linking (Persechini & Kretsinger, 1988), low-angle X-ray scattering (Heidorn & Trewhella, 1988), and NMR spectroscopy (Ikura et al., 1991) have been used to demonstrate the dynamic disorder of the central region of the bridging helix. The amphiphilic helix model [for a review, see O'Neil and DeGrado (1990)] for the structure of a peptide corresponding to the calmodulin-binding domain of the myosin light chain kinase when bound to CaM was first directly confirmed by NMR-based studies (Roth et al., 1991) and the structure of an entire complex subsequently characterized by both NMR (Ikura et al., 1992; Roth et al., 1992) and crystallographic (Meador et al., 1992) methods. Very little, however, is known about how calmodulin initially recognizes the domain, how it collapses from an initial encounter complex to the final compact state, or the energetics of these events and associated structural changes. In order to monitor the dynamics of the molecular recognition process, one could attempt to follow the kinetic events directly, as has recently been attempted using stopped-flow fluorescence spectroscopy [see the discussion by Török and Whitaker (1994)], or by quantitating the equilibrium manifold of states accessible to the complex. Hydrogen exchange methods in principle allow access to the equilibrium manifold of states and are employed here in our study of the energetics and dynamics of CaM in complex with a peptide corresponding to the calmodulin-binding domain of the smooth muscle myosin light chain kinase.

It now appears well established that solvent-catalyzed exchange of the amide hydrogens of proteins requires transient breakage of intraprotein hydrogen bonds to allow hydrogen bonding to solvent (Englander & Kallenbach, 1984). Given this basic physical mechanism, hydrogen exchange can therefore potentially provide detailed information about local dynamics and locally resolved free energy changes in proteins (Englander & Kallenbach, 1984). In principle, then, the hydrogen exchange behavior of the hydrogen-bonded amide hydrogens of the smMLCKp peptide bound to calmodulin can provide energetic information about the molecular recognition process. As is demonstrated here, hydrogen exchange can provide an unusually clear view of both the structural transformations and the associated energetics of the recognition of an unstructured peptide by calmodulin and the subsequent collapse to a compact complex.

MATERIALS AND METHODS

Sample Preparation. Calmodulin was expressed in *Escherichia coli* and purified by phenyl-Sepharose affinity chromatography (Gopalakrishna & Anderson, 1982; Seeholzer & Wand, 1989). An N-terminal acetylated and C-terminal amidated peptide corresponding to the smooth muscle myosin light chain kinase calmodulin-binding domain (Lukas et al., 1986; Kemp et al., 1986) was synthesized as described elsewhere (Roth et al., 1991). The sequence of the smMLCKp peptide used is acetyl-A-R-R-K-W-Q-K-T-G-H-A-V-R-A-I-G-R-L-S-NH_2. The peptide was synthesized with α-^{15}N-labeled alanine, lysine, valine, glycine, and leucine amino acids for a total of 9 labeled residues of the 19 of the peptide. Complexes between CaM and the peptide were prepared by titration under dilute conditions (Seeholzer & Wand, 1989). Except as noted, samples for NMR analysis contained, in a final volume of 0.55 mL, 1−4 mM calmodulin in a 10−20% molar excess over the smMLCKp peptide, 10 mM imidazole-d_4, 40 mM $CaCl_2$, and 100 mM KCl. The pH was varied from 5.9 to 8.6 as required. To monitor the exchange of H for D, the lyophilized CaM−smMLCKp preparations were hydrated with 100 μL of H_2O (to avoid refolding artifacts) followed by addition of D_2O to initiate exchange. To monitor the exchange of D for H, the lyophilized samples were hydrated with D_2O followed by addition of H_2O to initiate exchange.

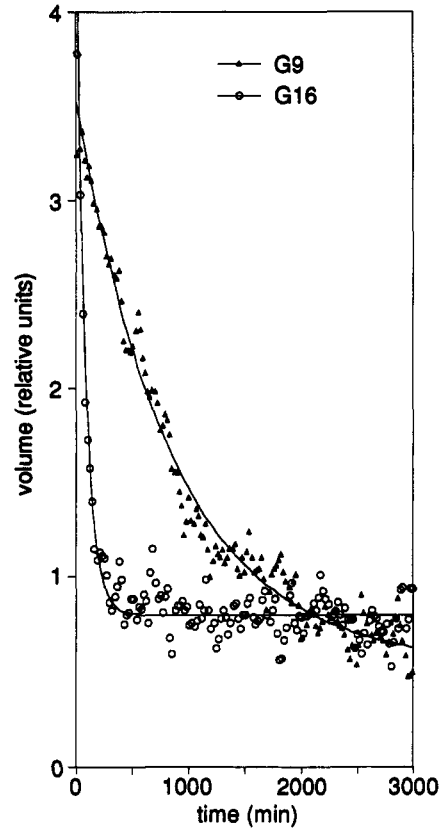

FIGURE 1: Examples of the method used to measure relatively slow amide hydrogen exchange rates at ^{15}N-labeled sites of the smMLCKp peptide bound to calcium-saturated calmodulin using ^{15}N−^{1}H correlation spectroscopy. Shown are the decays of the intensities of the amide ^{15}N−^{1}H cross peaks of Gly-9 and Gly-16 of the smMLCKp peptide bound to calmodulin in a set of serially acquired ^{15}N-HSQC NMR spectra upon dilution of a protonated sample into D_2O buffer at pH* 6.98. The observed rates are 1.2×10^{-3} min^{-1} and 1.3×10^{-2} min^{-1}.

NMR Spectroscopy. All NMR experiments were carried out on a Bruker AMX-500 NMR spectrometer at 298 K. Standard pulse sequences were used for direct, serial acquisition of ^{15}N-HSQC (Bodenhausen & Ruben, 1980) and ^{15}N-HSQC-NOESY (Clore et al., 1988) spectra. Saturation-transfer experiments utilized HSQC spectra obtained using spin locks for water suppression (Messerle et al., 1989) with or without direct presaturation of the water resonance. Reference high-resolution ^{15}N−^{1}H correlation spectra were derived from data sets composed of 128 complex points in the incremented time domain and 512 complex points in the acquisition time domain. Spectra used to quantitate hydrogen exchange were composed of 32 complex points in the incremented time domain and 512 complex points in the acquisition time domain. Sweep widths for the ^{1}H and ^{15}N dimensions were 6667 and 2016 Hz, respectively. The method of States−TPPI (Marion et al., 1989) was used to provide quadrature detection during the incremented time

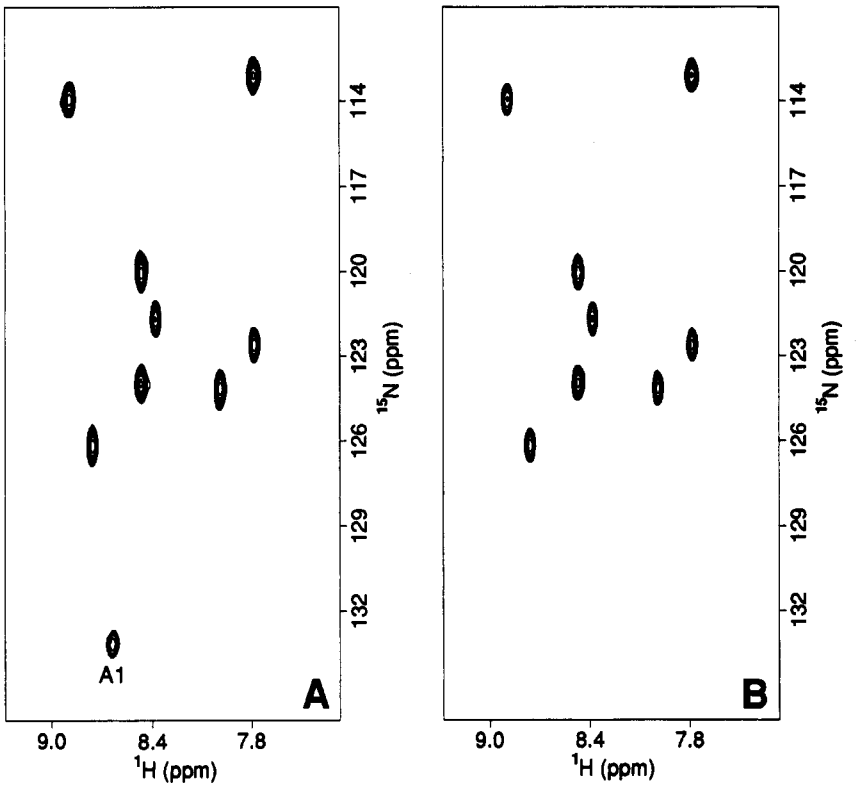

FIGURE 2: Determination of the rate of exchange of the amide hydrogen of Ala-1 by saturation transfer. ^{15}N-HSQC without saturation of solvent (panel A) and with saturation of solvent (panel B) shows the effects of saturation transfer to the amide hydrogen of Ala-1 which is in rapid exchange on the NMR time scale with solvent. These spectra were obtained at pH* 8.07 and 25 °C and when combined with similar spectra obtained at pH* 7.79 and 7.35 provide an estimate of the slowing factor for exchange.

domain. Sixty-four scans per free induction decay were acquired, and sequential data sets were composed of 64 scans and 32 complex points each. All spectra were processed using the software package FELIX (Biosym Technologies).

Calculation of Hydrogen Exchange Rates and Slowing Factors. Obtained hydrogen exchange rates were corrected for the small isotope effect based on the mole fraction of deuterium present (Bai et al., 1993). Slowing factors for a given set of solution conditions were calculated using the empirical factors of Bai et al. (1993). *N*-Methyl values were used to calculate the slowing factors for the N-acetylated Ala-1 of the peptide. As the charge state of His-10 in the hydrogen exchange competent state(s) is not directly known (though see Results), slowing factors involving this residue (i.e., His-10 and Ala-11) were calculated using empirical intrinsic factors for both the neutral and positively charged species, and the resulting range was taken as a limit of their accuracy.

RESULTS

A variety of NMR-based techniques were employed to measure the hydrogen exchange rates of the backbone amide hydrogens of 18 of the 19 amino acid residues of a peptide analogue of the smooth muscle myosin light chain kinase calmodulin-binding domain (smMLCKp) while bound to calcium-saturated calmodulin (CaM). Exchange rates spanning 6 orders of magnitude were measured using a battery of techniques which allowed determination of the exchange rates of both ^{15}N- and ^{14}N-bonded amide hydrogens of the bound smMLCKp peptide. Key to this approach is the ability to filter the ^{1}H spectrum on the basis of the presence of bonded ^{15}N nuclei. The heteronuclear ^{15}N−^{1}H correlation spectrum of the labeled peptide bound to calcium-saturated calmodulin has been assigned previously (Roth et al., 1991).

The nine ^{15}N-labeled amide sites of the smMLCK peptide allow for direct, selective detection of their bonded hydrogens even in the presence of ^{1}H resonances arising from amide and aromatic hydrogens due to calmodulin. In the case of relatively slow hydrogen exchange (rates < 0.04 min^{-1}), the exchange rate can be simply measured in "real time" by sequential acquisition of HSQC spectra following initiation of exchange by dilution of the protonated sample into D_2O buffer. The rate of exchange at a given amide site is then obtained from a simple single exponential fit of the integrated peak volumes as a function of exchange time. Typical examples of exchange of an amide hydrogen for a deuteron from solvent are shown in Figure 1. Exchange was initiated by dilution of an H_2O solution of the complex into the D_2O exchange buffer in order to avoid potential refolding artifacts from the lyophilized state. The use of serially acquired HSQC spectra employing spin locks for water suppression allowed the exchange rates at six of the nine labeled sites to be determined under the conditions employed. Essentially identical rates were determined using CaM to smMLCKp ratios of 1.1:1 and 2.2:1. This is important as in order to probe the dynamics of the bound smMLCKp peptide, the measured exchange rate must, of course, arise from events that occur in the bound state and not be contaminated by exchange from the free, random coil peptide. This condition can be satisfied by taking advantage of the high affinity (K_a ~10^9 M^{-1}) of the peptide for CaM. The concentration of *free* peptide when the CaM:smMLCKp ratio is 1.1:1 and the CaM concentration is millimolar will be at least an order of magnitude greater than when the CaM:smMLCKp ratio

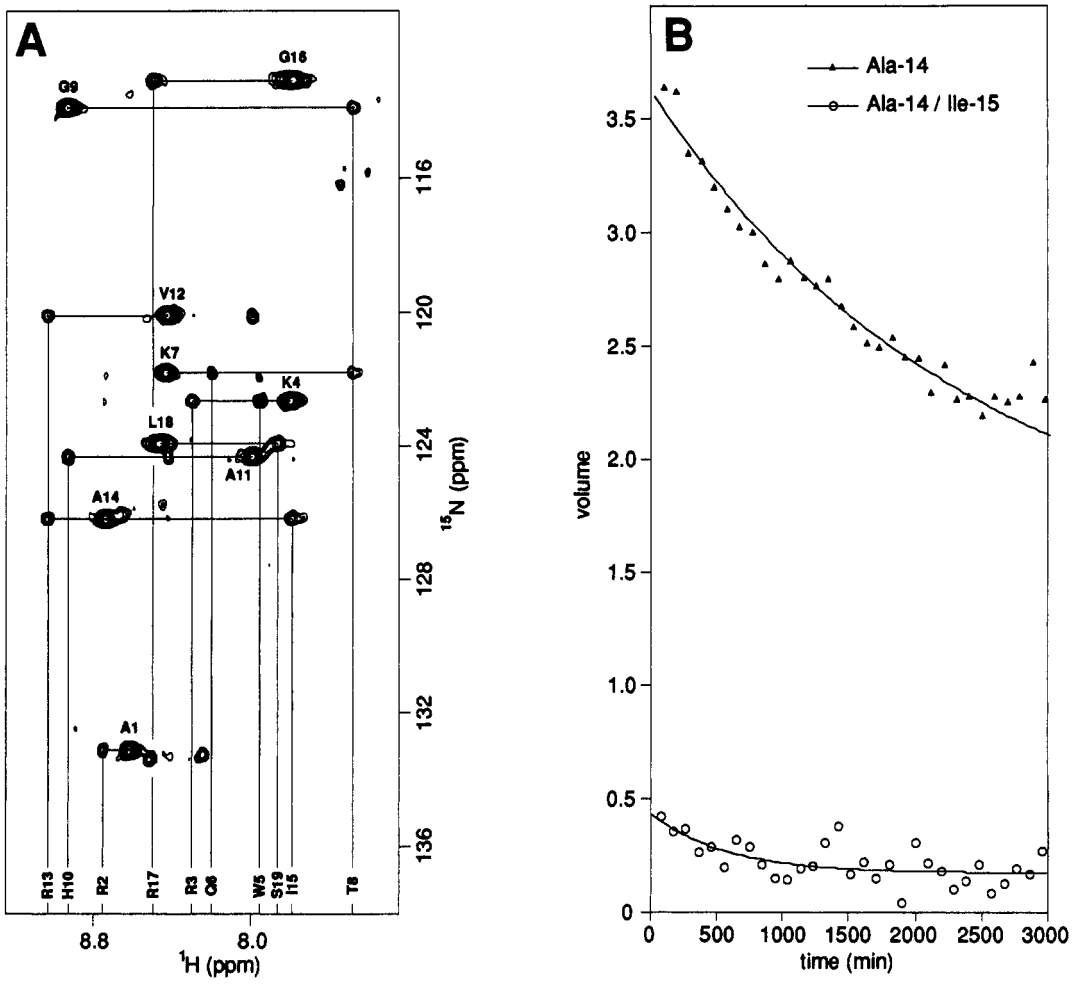

FIGURE 3: Examples of the method used to measure relatively slow amide hydrogen exchange rates at ^{14}N sites of the smMLCKp peptide bound to calcium-saturated calmodulin using ^{15}N−^{1}H correlation spectroscopy. The NOE cross peaks arising between adjacent amide hydrogens in the smMLCKp peptide bound to calmodulin are indicated in panel A and have been assigned previously (Roth et al., 1991). Panel B shows the decays of intensity of the Ala-14 ^{15}N−^{1}H autopeak and the Ile-15 ^{14}NH to Ala-14 ^{15}NH NOE cross peak in serially acquired HSQC-NOESY spectra collected with an NOE mixing time of 75 ms.

is 2.2:1. Hence, the fraction of time that a given amide NH will spend in the free peptide state will correspondingly decrease in the latter case. As the observed rate of exhange is the same under both conditions, the observed hydrogen exchange rates are indeed dominated by exchange from the *bound* state(s) of the peptide under the conditions employed here.

The rates of exchange of the amide hydrogens of Ala-1 and Lys-7 are too rapid to measure by the method of serial acquisition of HSQC spectra. The rate of exchange of the amide hydrogen of Lys-7 falls in the range that could be quantitated by serial acquisition of ^{15}N-filtered one-dimensional ^{1}H spectra. A sample of the complex was fully exchanged into D_2O, lyophilized, wetted with D_2O, and diluted into H_2O. At pH 5.94, Lys-7 is resolved in the ^{15}N-filtered ^{1}H spectrum from all but the very slowly exchanging amide of Val-12. The rate of exchange could then be determined from the increase in integrated intensity as a function of exchange time. The rate of exchange of the amide hydrogen of Ala-1 is even faster and was determined by saturation-transfer experiments undertaken at pH 7.35, 7.79, and 8.07 (Figure 2). Volumes of a given peak were measured in the absence (M_0) and the presence (M_{ps}) of water presaturation. The ratio of these volumes and an assumed average T_1 of 125 ms were used to calculate the exchange rate of the amide in question from eq 1 (Spera et al., 1991).

$$k = \frac{(M_0/M_{ps} - 1)}{T_1} \quad (1)$$

It should be noted that the generalized order parameters of the nine ^{15}N−^{1}H bonds of the bound smMLCKp peptide have been determined and found to be uniformly high across the full length of the peptide (Chen et al., 1993). Thus it is unlikely that variations in local dynamics would give rise to significant variation in the effective ^{1}H spin-lattice relaxations, making the assumption of a uniform effective T_1 reasonable.

Hydrogen exchange rates at slowly exchanging unlabeled amide nitrogen sites of the bound smMLCKp peptide were measured by following the decay of amide−amide NOEs involving one amide hydrogen at a ^{15}N-labeled site and another amide hydrogen at an unlabeled site in serially acquired ^{15}N-HSQC-NOESY spectra. Under the so-called EX_2 (Hvidt & Nielsen, 1966) conditions used here, the rate of exchange of the amide hydrogen of the unlabeled amino acid is equal to the rate of change in the NOE cross-peak volume minus the rate of change of the autocorrelation peak volume arising from the labeled amino acid in the ^{15}N-HSQC-NOESY spectrum. An example is shown in Figure 3. The use of NOE cross peaks in ^{15}N-HSQC-NOESY spectra to obtain hydrogen exchange rates is the least

Table 1: Solvent Exchange Rates and Slowing Factors of Amide Hydrogens of the smMLCKp Peptide Bound to Calcium-Saturated Calmodulin

residue	pH*	rate (min^{-1})	slowing factor[a]
Ala-1	7.35[b]	1.6×10^2	3.1
	7.79[b]	4.2×10^2	3.3
	8.07[b]	6.8×10^2	8.2
Arg-2	7.00[c]	5.4×10^2	2.3 (±1.4)
Arg-3	7.35[c]	5.4×10^2	8.5 (±5.1)
Lys-4	7.80[c]	5.4×10^2	$1.8\ (\pm 1.1) \times 10^1$
Trp-5	7.30[c]	5.4×10^2	1.9 (±1.2)
Gln-6	7.50[c]	5.4×10^2	5.3 (±3.2)
Lys-7	5.94[d]	$1.9\ (\pm 0.7) \times 10^{-2}$	$5.3\ (\pm 2.0) \times 10^3$
Thr-8	6.64[e]	$1.0\ (\pm 0.6) \times 10^{-2}$	$3.9\ (\pm 2.1) \times 10^4$
Gly-9	6.98[f]	$1.2\ (\pm 0.1) \times 10^{-3}$	$1.9\ (\pm 0.1) \times 10^6$
	6.64[e]	$4.3\ (\pm 0.3) \times 10^{-4}$	$2.4\ (\pm 0.2) \times 10^6$
	6.73[e]	$7.3\ (\pm 0.8) \times 10^{-4}$	$1.8\ (\pm 0.2) \times 10^6$
His-10	6.64[e]	$6.0\ (\pm 4.9) \times 10^{-3}$	$2.9\ (\pm 2.6) \times 10^5$
Ala-11	6.98[f]	$3.7\ (\pm 0.1) \times 10^{-3}$	$7.7\ (\pm 3.3) \times 10^5$
	6.64[e]	$4.3\ (\pm 0.2) \times 10^{-3}$	$3.4\ (\pm 1.8) \times 10^5$
	6.73[e]	$4.9\ (\pm 0.5) \times 10^{-3}$	$3.8\ (\pm 2.1) \times 10^5$
Val-12	8.07[f]	$2.7\ (\pm 0.4) \times 10^{-3}$	$7.0\ (\pm 1.0) \times 10^5$
Arg-13	6.73[e]	$5.7\ (\pm 2.3) \times 10^{-4}$	$6.7\ (\pm 2.7) \times 10^5$
Ala-14	6.98[f]	$7.7\ (\pm 0.4) \times 10^{-4}$	$1.7\ (\pm 0.1) \times 10^6$
	6.64[e]	$1.3\ (\pm 0.4) \times 10^{-3}$	$4.6\ (\pm 1.4) \times 10^5$
	6.73[e]	$4.2\ (\pm 0.6) \times 10^{-4}$	$1.8\ (\pm 0.2) \times 10^6$
Ile-15	6.73[e]	$1.3\ (\pm 0.5) \times 10^{-3}$	$6.2\ (\pm 2.5) \times 10^4$
Gly-16	6.98[f]	$1.3\ (\pm 0.1) \times 10^{-2}$	$6.6\ (\pm 0.4) \times 10^4$
	6.64[e]	$6.5\ (\pm 0.6) \times 10^{-3}$	$6.0\ (\pm 0.5) \times 10^4$
Arg-17	6.64[e]	$1.1\ (\pm 0.6) \times 10^{-2}$	$5.9\ (\pm 3.1) \times 10^4$
Leu-18	6.98[f]	$3.6\ (\pm 0.6) \times 10^{-2}$	$9.6\ (\pm 1.7) \times 10^3$

[a] Individual slowing factors were calculated using factors from Bai et al. (1993) as described in Materials and Methods. The average slowing factors used in Figure 5 were determined by the simple average of individual slowing factors. The error in the average slowing factors used in Figure 5 was determined from the maximum errors of the individual slowing factors. For Ala-11, consideration of the ambiguity of the charge state of the side chain of His-10 resulted in a slightly larger error in the average slowing factor used. For hydrogen exchange rates determined by chemical exchange effects, the given error in slowing factor includes uncertainity in the effective spin−lattice rates. See Figure 4 and the text for details. [b] This rate was determined by direct saturation transfer (see Figure 2). [c] These rates were determined by following exchange effects on the NOE cross-peak intensities in HQSC-NOESY spectra over the pH* range 6.31−8.59 as shown in Figure 4. The given pH* is that at which the exchange rate required to reduce the peak intensity to half its slow exchange value is achieved. [d] This rate was determined by serial acquisition of ^{15}N-filtered one-dimensional ^1H spectra. [e] These rates were determined by the serial acquisition of HSQC-NOESY spectra (see Figure 3). [f] These rates were determined by serial acquisition of HSQC spectra (see Figure 1).

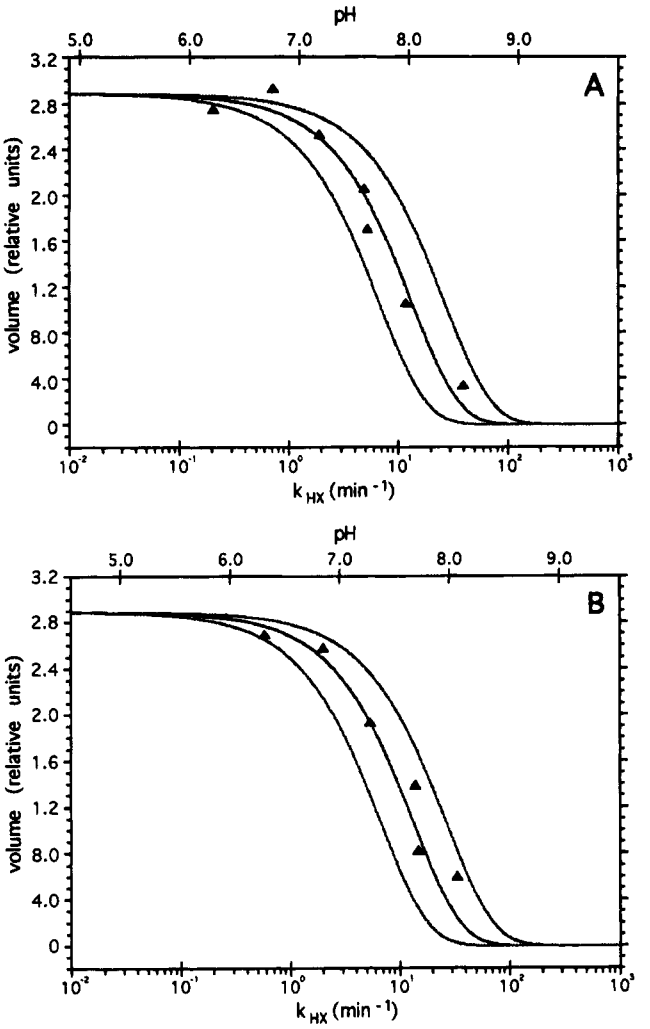

FIGURE 4: Examples of the method used to measure relatively fast amide hydrogen exchange rates at ^{14}N sites of the smMLCKp peptide bound to calcium-saturated calmodulin using $^{15}N-^1H$ correlation spectroscopy. Shown are the intensities of the Lys-4 $^{15}N-^1H$ autopeak (panel A) and Lys-4 ^{15}NH to Trp-5 ^{14}NH NOE cross peak as a function of pH. The effective rate for exchange is also shown on the lower abscissa. The center line is the best fit to the data, and the outer lines are calculated using the assumed error on the fitted rate and illustrate the conservative nature of the estimate.

sensitive of the techniques employed here. Comparison of the behavior of two cross peaks to an unlabeled amide NH flanked by two labeled amide NH's indicates that rates determined by this method can vary by up to 2-fold. Finally, the kinetic behavior of the "auto" peaks of the ^{15}N-HSQC-NOESY spectra compare favorably with the decay rates obtained using serially acquired ^{15}N-HSQC spectra (see Table 1).

To measure fast exchange rates at unlabeled amide sites, ^{15}N-HSQC-NOESY spectra were collected at pH values ranging from 6.31 to 8.59. The rate of exchange at the labeled Lys-4 site was also determined in this manner. An NOE mixing time of 75 ms was employed, which is in the linear region of the NOE-buildup curves at 500 MHz. A simple two-spin relaxation matrix was used to model the effects of saturation transfer over a range of conditions and relaxation time constants. For a two-spin case, analytical solutions are available for the eigenvalues and vectors of the relaxation matrix, making simulations facile. The effect of chemical exchange enters into the the diagonal terms of the rate matrix (Macura & Ernst, 1980). Using the standard expressions relating pH to the rate of hydrogen exchange and the recently recalibrated empirical factors for local sequence dependence (Bai et al., 1993), reasonably precise estimates of the effective exchange rate can be determined by fitting the observed cross-peak intensities as a function of pH. Very generous allowances for the imprecision of estimates of the intrinsic spin−lattice and cross-relaxation rates have only modest effects on the accuracy of the obtained hydrogen exchange rates. Examples are shown in Figure 4.

It should be noted that the rates of exchange of the slowly exchanging amides follow the predicted pH dependence over the range of pH used, indicating that exchange is occurring under the so-called EX_2 condition and, importantly, that the complex is structurally unaffected by the range of solution conditions employed.

Slowing factors for 18 of the 19 amide sites of the bound smMLCKp peptide were calculated using observed hydrogen

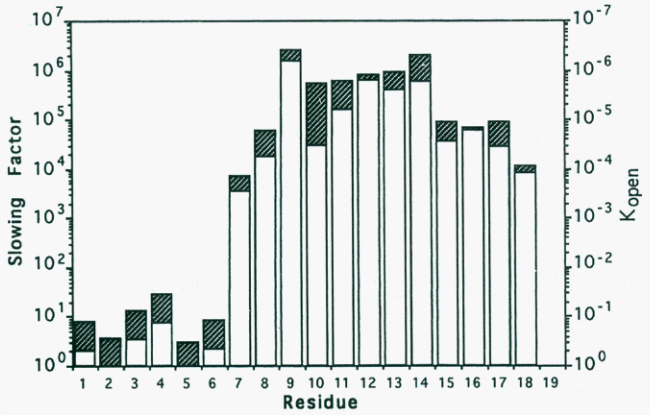

FIGURE 5: Slowing factors of the hydrogen exchange of the backbone amide hydrogens of the smMLCKp peptide bound to calcium-saturated calmodulin. Shaded regions of the histogram correspond to the experimental error of the underlying measurement. The rate expected for a free peptide was divided by the observed hydrogen exchange rate under identical solution conditions. The free peptide rate was calculated using the empirical factors due to Bai et al. (1993) and using the *N*-methyl value for the N-terminal acetyl group of the peptide. The uncertainity in the slowing factors of His-10 and Ala-11 also reflects uncertainity of the charge state of the histidine side chain in the hydrogen exchange competent state(s). The minimum and maximum rates calculated using the neutral and positively charged species were used to define the minimum and maximum values for the free peptide rate.

exchange rates obtained (Table 1) using the various approaches summarized above and the rates predicted for the free, unstructured peptide according to the empirical factors due to Bai et al. (1993). Shaded regions of the histogram shown in Figure 5 correspond to the experimental uncertainty and are determined from up to three independent measurements. In the case of His-10 and Ala-11, the shaded regions of the histogram also include the effects of uncertainty in the charge state of the histidine side chain in the hydrogen exchange competent state(s). It should be mentioned, however, that the general pH dependence of the hydrogen exchange rates of His-10 and Ala-11 is consistent with a pK_a of ~6.5−7 for the histidine side chain in the exchange-competent state(s). The exchange rate of Ser-19 could not be accurately determined due to spectral degeneracies that occur at the low pH necessary to accurately estimate the rate.

DISCUSSION

It is now well established that solvent-catalyzed exchange of the amide hydrogens of proteins requires transient breakage of intraprotein hydrogen bonds to allow sufficient hydrogen bonding to solvent to promote exchange (Englander & Kallenbach, 1984). Given this basic physical requirement, hydrogen exchange can therefore potentially provide detailed information about local dynamics and locally resolved free energy changes in proteins (Englander & Kallenbach, 1984). The smMLCKp−CaM complex is well-suited for study by this technique from several important points of view. The structure of the bound peptide is well characterized by both crystallographic and NMR-based methods (Roth et al., 1991; Meador et al., 1992). The structure determined by NMR methods indicates that the first intrahelical hydrogen-bonded amide hydrogen of the bound peptide is that of Lys-7 (Roth et al., 1991). This is consistent with the present observationthat the amide hydrogens of residues 1−6 of the bound smMLCKp peptide have slowing factors approaching unity. This also implys that solvent can easily penetrate to the

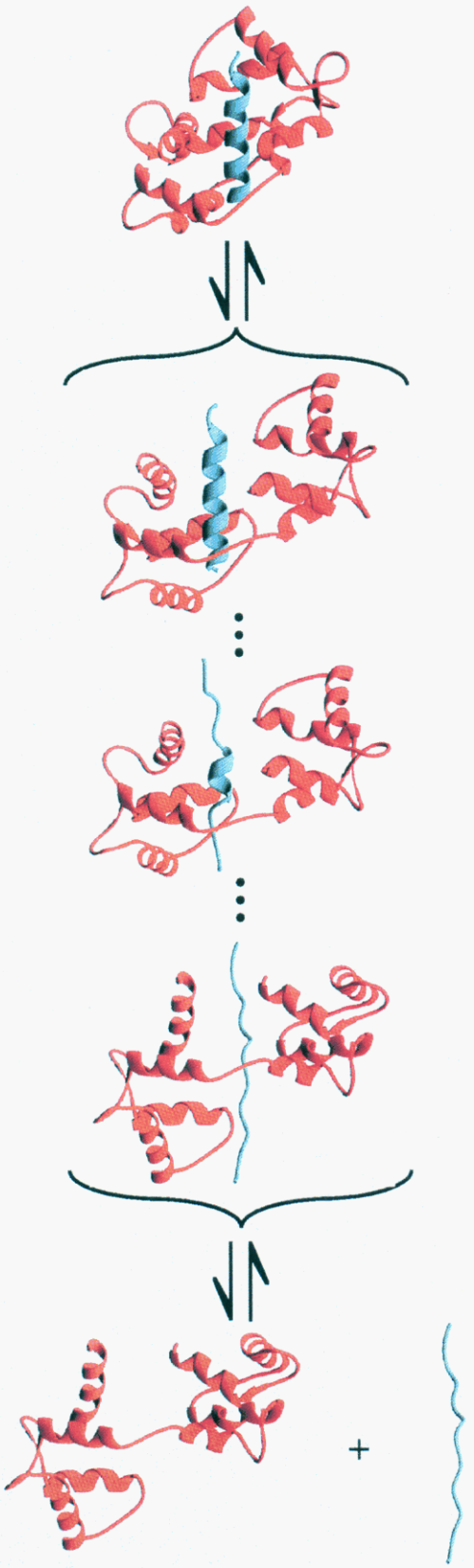

FIGURE 6: Schematic illustration of the physical model used to interpret the observed hydrogen exchange of the smMLCKp peptide bound to calmodulin. The random coil peptide forms an initial encounter complex with an open dumbbell-like calmodulin structure. The general surface interactions promote helix−coil transitions which lead to the formation of the helix on the surface of the protein. This manifold of states is characterized by an effective free energy difference between the least and most stable hydrogen bond of about 2.5 kcal/mol. The complete helix provides properly oriented contacts to allow for the collapse of the complex. This latter reorganization is characterized by a free energy change of about 5.5 kcal/mol. Drawn with Ribbons (Carson, 1987).

backbone of the first six residues. The slowing factors for the hydrogen-bonded amide NH at the ends of the helical segment are about 10^4. The largest slowing factors, which comprise the plateau region in Figure 5 and include residues 10−14, are on the order of 10^6. The decrease in slowing factors on both the N- and C-terminal sides of the central plateau is, on average, about a factor of 2.5 per residue. It should be noted that for heterogeneous amino acid sequences the decrease in hydrogen bond stability toward the ends of a helical segment is not expected to be smooth, even for model peptides in water (see below). This roughness or "fine structure" can also potentially be due to local structural interactions. Thus, the apparently high slowing factor for the amide hydrogen of Gly-9 is suggestive of modest protection in the hydrogen exchange competent states discussed in detail below.

The general dependence of the slowing factors obtained for the bound smMLCKp peptide as a function of sequence position is characteristic for hydrogen bond breakage arising from helix−coil transitions. Such transitions lead to "end fraying" and result in more stable helical hydrogen bonding toward the center of the peptide. The helix−coil transition for isolated helices is often treated in a statistical mechanical way utilizing the models of Zimm and Bragg (1959) or Lifson and Roig (1961). With such treatments, one can calculate the fraction of time a given amide NH is hydrogen bonded given residue-specific parameters of the model (S and σ for Zimm−Bragg). For model peptides in water, most individual amino acids generally have S values between 0.5 and 2.0 [see, for example, Lyu et al. (1990) and Rohl and Baldwin (1994)]. The apparent S value is a reflection of the effective hydrogen bond stability which in turn is manifested in the hydrogen exchange slowing factors. For proteins, such as cytochrome c, observed patterns of hydrogen exchange slowing factors of helical segments indicate effective S parameters on the order of 10 or larger (Wand et al., 1986). Such large effective S values are indicative of extensive interactions between the helix and surrounding protein.

It is important to note then that the observed end fraying of the bound smMLCKp peptide results in a relatively *small* range of slowing factors, indicating low effective S values. This is most consistent with exchange arising from helix−coil transitions in a relatively unhindered state, perhaps suggesting that exchange occurs in the free peptide state. However, this is clearly not the case, as shown above. In addition, the slowing factors at the ends of the helical segment are very large, on the order of 10^4. Such large values for the ends of helical segments of free peptides are not predicted by small S parameters. The physical explanation of these observations is outlined schematically in Figure 6. Given the range of effective S values reflected in the slope of the end fraying, one can model the helix−coil transition such that a range of 10^2 in slowing factors is predicted using nucleation (σ) parameters on the order of 10^{-3}, a value which is seen in model peptides (Rohl et al., 1992; Rohl & Baldwin, 1994). If the helix−coil manifold is considered the only set of states from which hydrogen exchange can occur (i.e., they provide the dominant structural reorganizations that lead to transient hydrogen bond breakage and exposure of the amide NH to solvent), then initial slowing factors of 10^4 require that there be a major reorganization that moves the complex from one that suppresses the helix−coil transitions to one that allows them to occur with parameters characteristic of a relatively unhindered peptide (i.e., extensively solvated but bound). This picture leads to a model where this equilibrium results in an opening of the complex such that the peptide is brought to the surface of calmodulin and extensively exposed to solvent. The observed hydrogen exchange slowing factors require that this equilibrium be characterized by an equilibrium constant of 10^4 ($\Delta G \sim 5.5$ kcal/mol). The pattern of slowing factors indicates that helix−coil transitions in the peptide occur in the reorganized state of the complex. In the reorganized state, the peptide is extensively solvated, and the helix−coil transitions create a manifold of states leading to transient breakage of intrahelical hydrogen bonding, allowing for exchange of amide hydrogens with solvent. This manifold is characterized by an effective equilibrium constant spanning the least and most protected amide NH of $\sim 10^2$ (corresponding to a ΔG of ~ 2.5 kcal/mol). The reorganized complex is in direct equilibrium with the dissociated complex. When this process is viewed in reverse, a free energy scale is revealed for the binding of the unstructured free peptide to calmodulin followed by the induction of helical structure and collapse to the compact complex. This view is consistent with the results for the binding of a D-amino acid analogue of the smMLCKp peptide to CaM in which collapse to the compact complex is frustrated but induction of helical structure on the surface of calmodulin is essentially complete (Fisher et al., 1994). In a kinetic sense, the collapse to the compact complex would presumably be associated with a relatively large barrier and may in fact be the source of biphasic behavior described in a preliminary report of a stopped-flow fluorescence study of the binding kinetics of a related peptide (Török & Whitaker, 1994).

In summary, the results presented here provide a unique view of the energetics and dynamics of the molecular recognition of a peptide ligand by calmodulin and help to unify our understanding of both the static and dynamic aspects of this high-affinity interaction. Since a number of signal tranduction pathways involve the binding of small protein domains, the approach illustrated here may be of general use in delineating the energetics and intermediates of molecular recognition by these proteins.

ACKNOWLEDGMENT

We are grateful to Professor S. Walter Englander for helpful discussion.

REFERENCES

Babu, Y. S., Bugg, C. E., & Cook, W. J. (1988) *J. Mol. Biol. 204*, 191−204.
Bai, Y., Milne, J. S., Mayne, L., & Englander, S. W. (1993) *Proteins 17*, 75−86.
Bodenhausen, G., & Ruben, D. (1980) *J. Chem. Phys. 69*, 185−189.
Carson, M. (1987) *J. Mol. Graphics 5*, 103−106.
Chen, C., Feng, Y., Short, J. H., & Wand, A. J. (1993) *Arch. Biochem. Biophys. 306*, 510−516.
Clore, G. M., Bax, A., Wingfield, P., & Gronenborn, A. M. (1988) *FEBS Lett. 238*, 17−21.
Englander, S. W., & Kallenbach, N. R. (1984) *Q. Rev. Biophys. 16*, 521−655.
Fisher, P. J., Prendergast, F. G., Ehrhardt, M. R., Urbauer, J. L., Wand, A. J., Sedarous, S. S., McCormick, D. J., & Buckley, P. J. (1994) *Nature 368*, 651−653.

Gopalakrishna, R., & Anderson, W. B. (1982) *Biochem. Biophys. Res. Commun. 104*, 830−836.
Heidorn, D. B., & Trewhella, J. (1988) *Biochemistry 27*, 909−915.
Hvidt, A., & Nielsen, S. O. (1966) *Adv. Protein Chem. 21*, 287−386.
Ikura, M., Spera, S., Barbato, G., Kay, L. E., Krinks, M., & Bax, A. (1991) *Biochemistry 30*, 9216−9228.
Ikura, M., Clore, G. M., Gronenborn, A. M., Zhu, G., Klee, C. B., & Bax, A. (1992) *Science 256*, 632−638.
Kemp, B. E., Pearson, R. B., Guerriero, V., Jr., Bagchi, I. C., & Means, A. R. (1987) *J. Biol. Chem. 262*, 2542−2548.
Lifson, S., & Roig, A. (1961) *J. Chem. Phys. 34*, 1963−1974.
Lukas, T. J., Burgess, W. H., Prendergast, F. G., Lau, W., & Watterson, D. M. (1986) *Biochemistry 25*, 1458−1464.
Lyu, P. C., Liff, M. I., Marky, L. A., & Kallenbach, N. R. (1990) *Science 250*, 669−673.
Macura, S., & Ernst, R. R. (1980) *Mol. Phys. 41*, 95−117.
Marion, D., Ikura, M., Tschudin, R., & Bax, A. (1989) *J. Magn. Reson. 85*, 393−399.
Meador, W. E., Means, A. R., & Quiocho, F. A. (1992) *Science 257*, 1251−1255.
Messerle, B. A., Wider, G., Otting, G., Weber, C., & Wüthrich, K. (1989) *J. Magn. Reson. 85*, 608−613.
O'Neil, K. T., & De Grado, W. F. (1990) *Trends Biochem. Sci. 15*, 59−64.
Persechini, A., & Kretsinger, R. H. (1988) *J. Biol. Chem. 263*, 12175−12178.
Rohl, C. A., & Baldwin, R. L. (1994) *Biochemistry 33*, 7760−7767.
Rohl, C. A., Scholtz, J. M., York, E. J., Stewart, J. M., & Baldwin, R. L. (1992) *Biochemistry 31*, 1263−1269.
Roth, S. M., Schneider, D. M., Strobel, L. A., VanBerkum, M. F. A., Means, A. R., & Wand, A. J. (1991) *Biochemistry 30*, 10078−10084.
Roth, S. M., Schneider, D. M., Strobel, L. A., VanBerkum, M. F. A., Means, A. R., & Wand, A. J. (1992) *Biochemistry 31*, 1443−1451.
Seeholzer, S. H., & Wand, A. J. (1989) *Biochemistry 28*, 4011−4020.
Spera, S., Ikura, M., & Bax, A. (1991) *J. Biomol. NMR 1*, 155−165.
Török, K., & Whitaker, M. (1994) *BioEssays 16*, 221−224.
Wand, A. J., Roder, H., & Englander, S. W. (1986) *Biochemistry 25*, 1107−1114.
Zimm, B. H., & Bragg, J. K. (1959) *J. Chem. Phys. 31*, 526−535.

BI942762A